
DISSERTATION

COLORADO STATE UNIV'S THESIS TEMPLATE

Submitted by
Matthew Gregory Hogan
Department of Physics

In partial fulfillment of the requirements
For the Degree of Doctor of Philosophy
Colorado State University
Fort Collins, Colorado
Summer 2019

Doctoral Committee:

Advisor: Walter Toki
Co-Advisor: Robert Wilson

Norman Buchanan
Wen Zhou

Copyright by Matthew Gregory Hogan 2019
All Rights Reserved

ABSTRACT

COLORADO STATE UNIV'S THESIS TEMPLATE

This document aims to get you started typesetting your thesis or dissertation in \LaTeX .

ACKNOWLEDGEMENTS

I would like to thank the Elliott Forney for making a publicly accessible L^AT_EX template

TABLE OF CONTENTS

ABSTRACT	ii
ACKNOWLEDGEMENTS	iii
LIST OF TABLES	v
LIST OF FIGURES	vi
Chapter 1 Introduction	1
1.1 Introduction to Neutrinos	2
1.1.1 Neutrinos in the Standard Model	3
1.1.1.1 Neutrino Weak Interactions	5
1.1.1.2 Chirality	5
1.1.2 Neutrino Oscillations	9
1.1.2.1 Two Flavor Derivation	10
1.1.2.2 Three Flavor Oscillations	13
1.1.2.3 Matter Effects	18
1.1.3 CP Violation: Origins of Matter	19
1.2 Tokai-to-Kamioka Experiment	20
1.2.1 Neutrino Production at J-PARC	21
1.2.2 T2K Near Detectors	25
1.2.3 Far Detector: Super-Kamiokande	25
1.2.4 Oscillation Analysis	25
Bibliography	27

LIST OF TABLES

1.1	Sensitivity of Different Oscillation Experiments	15
1.2	Table of Best Fit MNSP Parameters Split by Normal and Inverted hierarchy . .	17

LIST OF FIGURES

1.1	The Standard Model of particle physics	4
1.2	CC And NC Feynman Diagrams	6
1.3	Helicity of Neutrino Through Decay of Charged Pi Mesons	8
1.4	Depiction of Two Neutrino Flavor Change of Basis	11
1.5	Survival and Disappearance Probability	13
1.6	Logarithmic Plot of the Two Flavor Survival Probability	14
1.7	Mass hierarchy Problem And MNSP Representation	18
1.8	Birds eye view of the T2K experiment on the Japanese archipelago	21
1.9	Bird's eye view of the J-PARC center	22
1.10	Schematics of the J-PARC Accelerators	23
1.11	The neutrino beamline at J-PARC	24
1.12	T2K Accumulated Protons on Target	25

Chapter 1

Introduction

Chose trop vue n'est chère tenue

A thing too much seen is little prized

French proverb

This describes the thesis

1.1 Introduction to Neutrinos

The history of the neutrino can be traced back to electron energy spectrum observed in neutron β -decay. While measurements of α - and γ -decay of atomic nuclei showed discrete spectral lines, the electron (β particle) exhibited a continuous energy spectrum. Experimentally, there were two observed particles in each decay process and classical physics dictated that the outgoing daughter particles should have discrete energies. The fact that the β -decay spectrum was not this way posed a fundamental problem for physicists in the mid-1910s and later, was energy conserved? Two solutions were postulated: either the “energy conservation law is only valid statistically in such a process [...] or an additional undetectable new particle [...] carrying away the additional energy and spin [...] is emitted [21].” The latter solution was supported by Wolfgang Pauli in a letter dated 4 December 1930 to a group of physicists meeting in Tübingen, modern Germany, where he first proposed what we would call a neutrino today¹. Pauli’s solution also predicted that the undetected neutrino would have half-integer spin, a quantum mechanical property of matter, since the observed particles in β -decay did not conserve angular momentum. The existence of the neutrino and validation of Pauli’s predictions would not experimentally verified for another 20 years.

The neutrino was first discovered in 1953 by Clyde Cowan and Frederick Reines using a nuclear reactor in South Carolina, U.S.A.. Since then three types of neutrinos have been observed and from unique sources like the Sun and a supernova. Neutrino physics continues to be an active region of physics since neutrinos are unique probes to processes otherwise inaccessible in laboratories. For instance in the depths of the Sun’s core where fusion occurs

¹In W Pauli’s December 1930 letter, he referred to his proposed particle as the “neutron”, which is not the same neutron we know of today. At that point in time, the neutral particles inside the atomic nucleus, also called “neutrons”, had not been discovered, let alone understood. The neutron, which was discovered in 1932 by James Chadwick, has been formally associated as the neutral, cousin particle to the proton. It would be Enrico Fermi who would coin the particle in W Pauli’s letter and solution to the β -decay spectrum a “neutrino”, meaning *little neutral one*.

and neutrinos are created, neutrinos are able to travel through the ultra dense and hot medium of the core (over 10^7 degrees Kelvin) and outer layers of the Sun and reach us on Earth.

Neutrinos rarely interact with normal matter, meaning that they travel essentially unimpeded towards one's particle detector. The rarity of such interactions can be illustrated with the fact that given nearly 7.0×10^{10} neutrinos/cm²/sec² are incident on the Earth from the Sun, statistically one solar neutrino can harmlessly interact with an individual. So this begs the question: how does one detect a neutrino? The short answer is one needs a ultra large volume of matter and a large enough flux of neutrinos in its path just to detect one given today's technology.

Scientists continue to be interested in neutrinos due to properties they exhibit. One of the more recent and surprising aspects about neutrinos is their ability to undergo “flavor oscillations” where a neutrino of definite flavor (type) is created and later observed as a different flavor. The impact of such oscillations could help explain the observed matter and anti-matter asymmetry in the Universe.

1.1.1 Neutrinos in the Standard Model

The Standard Model (SM) of particle physics is the theory that describes the electromagnetic, strong nuclear, and weak nuclear forces and the elementary particles therein. These three forces and the gravitational force constitute the four *known* fundamental forces of the Universe. Each force in the SM has at least one “force carrier” particle that mediates the interactions between particles. The force carriers are formally called “gauge bosons” which indicates they are particles with integer (0, 1, 2, ...) spin that come in temporary but unobservable existence to mediate the interaction. The weak nuclear bosons, the charged W^\pm and neutral Z, couple to neutrinos as well as the other fermions, particles with half-integer

²To give some perspective to this number, this means 70 billion neutrinos are travelling every second through an area similar to one's own thumb nail.

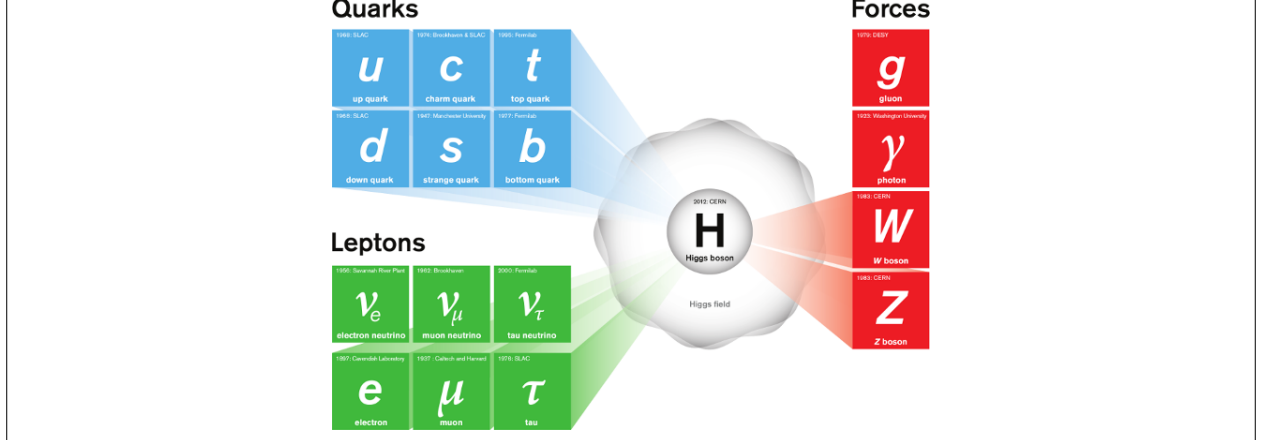


Figure 1.1: The Standard Model of particle physics consists of six quarks (up, down, strange, charm, bottom, and top), six leptons (electron, muon, tau, electron neutrino, muon neutrino, and tau neutrino), four force propagating bosons (gluon, photon, W, and Z), and the Higgs boson. The quarks, electron, muon, tau, W, and Z all gain mass through the Higgs field. The focus of this thesis are the neutrinos which are classified according to their charged, more massive Lepton cousins. Image taken from [4].

$(\frac{1}{2}, \frac{3}{2}, \frac{5}{2}, \dots)$ spin, in the SM. All the elementary particles of the SM are shown in Figure 1.1 on page 4 .

Neutrinos in the SM are electrically neutral, massless particles categorized into three generations based on their charged, more massive Lepton cousins. The neutrino and charged lepton pair into a “weak isospin doublet” in the SM. These doublets are locally gauge invariant under a $SU(2) \times U(1)$ symmetry which leads to the required existence of the photon and W and Z bosons³.

What follows is a brief introduction to neutrino interactions as well as some of their fundamental properties.

³A gauge theory describes ways to measure physical forces or fields through interactions between elementary particles. The electric or magnetic fields for example can only be probed by charged particles. In the realm of quantum field theories, fields are postulated to permeate everywhere and it is excitations of these fields which produce experimental observables. Fields are constructed using the Lagrangian formalism and altered using gauge transformations. If altering the Lagrangian in some way does not affect the observables, this is referred to as a gauge invariance. Local gauge invariance means that under the constraints of the experiment, certain gauge transformations do not affect the observables. The allowed locally gauge invariant transformations require knowledge of its underlying Lie, or symmetry, group. With the weak isospin doublets, the Lie groups are $SU(2) \times U(1)$ where $SU(2)$ is the special unitary group of 2×2 unitary matrices, and $U(1)$ is the unitary (circle) group consisting of complex numbers of magnitude 1.

1.1.1.1 Neutrino Weak Interactions

The name “weak force” comes from the fact that this force has a much smaller effective range than the electromagnetic and strong nuclear forces. This is due to the weak mediating bosons, the W and Z, being massive particles unlike the massless gluon (g) and photon (γ). The W/Z have masses of 80/90 GeV/c², which is more massive than all the elementary particles except for the top quark. For weak interactions to occur at energies far below the masses (also called “off-shell”) of the W and Z, the interaction time must be infinitesimally small as dictated by the Heisenberg Uncertainty Principle

$$\Delta E \Delta t \gtrsim \hbar \quad (1.1)$$

where ΔE is the energy of the particle and Δt is the time which the particle exists.

Weak interactions are classified into two classes: charged current (CC) and neutral current (NC). CC interactions involve one of the two charged W bosons and change the incoming neutrino of flavor ν_l ($l = e, \mu, \tau$) into an electrically charged lepton of flavor l or vice-versa. The same cannot be said of NC interactions which exchange a neutral Z boson. NC interactions do not change the flavor of the incoming particles and are therefore flavor agnostic. An example of each interaction type is shown in Figure 1.2 on page 6 .

1.1.1.2 Chirality

Neutrinos are believed to follow the free-particle Dirac Equation which is given by

$$\left[i\hbar \sum_{\mu=0}^3 \gamma^\mu \partial_\mu - mc \right] \psi = 0 \quad (1.2)$$

where

$$\gamma^0 = \begin{bmatrix} I_2 & 0 \\ 0 & -I_2 \end{bmatrix}, \gamma^1 = \begin{bmatrix} 0 & \sigma_x \\ -\sigma_x & 0 \end{bmatrix}, \gamma^2 = \begin{bmatrix} 0 & \sigma_y \\ -\sigma_y & 0 \end{bmatrix}, \gamma^3 = \begin{bmatrix} 0 & \sigma_z \\ -\sigma_z & 0 \end{bmatrix}, \quad (1.3)$$

I_2 is the 2×2 identity matrix, $\sigma_{x,y,z}$ are the Pauli Spin matrices, and

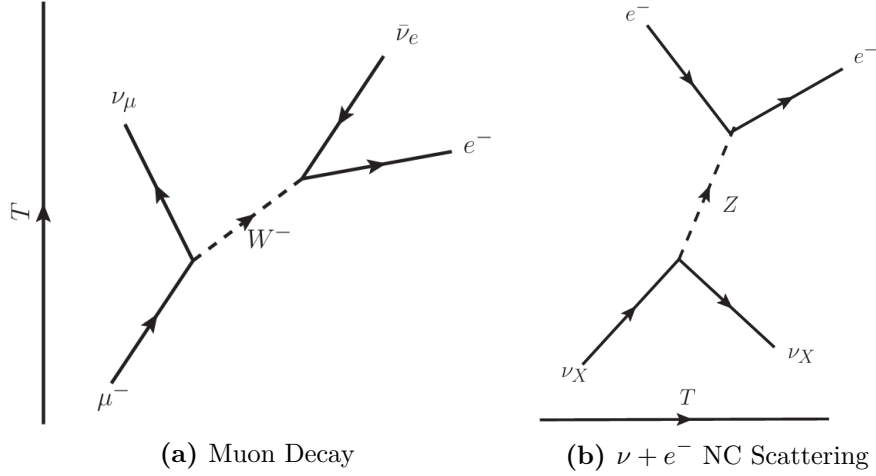


Figure 1.2: Left: Muon decay ($\mu^- \rightarrow \nu_\mu \bar{\nu}_e e^-$) Feynman diagram with time increasing from bottom to top. This is a charged current process that converts a muon into a muon neutrino via the emission of a W boson. Due to a conserved quantum number called lepton number, the W must emit an electron and electron neutrino pair. Right: Neutral current interaction Feynman diagram where time increases from left to right. This is a neutral current interaction where a neutrino of arbitrary flavor X scatters off an electron via the emission of a Z boson.

$$\partial_0 = \frac{1}{c} \frac{\partial}{\partial t}, \partial_1 = \frac{\partial}{\partial x}, \partial_2 = \frac{\partial}{\partial y}, \partial_3 = \frac{\partial}{\partial z}. \quad (1.4)$$

The solutions to (1.2) are called Dirac spinors and can be written in terms of left-handed (LH) and right-handed (RH) components. Any spinor can be decomposed in LH and RH projections using a “chiral” operator \hat{O} as

$$\psi = (\hat{O}_{\text{LH}} + \hat{O}_{\text{RH}}) \psi. \quad (1.5)$$

The chiral operators $\hat{O}_{\text{LH,RH}}$ in (1.5) are defined as

$$\hat{O}_{\text{LH}} \psi = \frac{1}{2} (I_4 - \gamma^5) \psi = \psi_{\text{LH}} \quad \hat{O}_{\text{RH}} \psi = \frac{1}{2} (I_4 + \gamma^5) \psi = \psi_{\text{RH}} \quad (1.6)$$

where I_4 is the 4×4 identity matrix,

$$\gamma^5 = i\gamma^0\gamma^1\gamma^2\gamma^3 = \begin{bmatrix} 0 & I_2 \\ I_2 & 0 \end{bmatrix}, \quad (1.7)$$

and $\psi_{\text{LH,RH}}$ are LH and RH chiral spinors. Using (1.6), the Dirac Equation then becomes after some manipulation

$$\begin{aligned} i\hbar \left(\frac{1}{c} \frac{\partial}{\partial t} - \boldsymbol{\sigma} \cdot \boldsymbol{\nabla} \right) \psi_{\text{RH}} &= m\gamma^0 \psi_{\text{LH}} \\ i\hbar \left(\frac{1}{c} \frac{\partial}{\partial t} + \boldsymbol{\sigma} \cdot \boldsymbol{\nabla} \right) \psi_{\text{LH}} &= m\gamma^0 \psi_{\text{RH}}, \end{aligned} \quad (1.8)$$

where

$$\boldsymbol{\sigma} \cdot \boldsymbol{\nabla} = \sum_{i=1}^3 \sigma_i \nabla_i. \quad (1.9)$$

In the limiting case of vanishing mass ($m \rightarrow 0$), as in the SM, the free particle equations decouple into

$$\begin{aligned} \left(\frac{E}{c} - \boldsymbol{\sigma} \cdot \mathbf{P} \right) \psi_{\text{RH}} &= 0 \\ \left(\frac{E}{c} + \boldsymbol{\sigma} \cdot \mathbf{P} \right) \psi_{\text{LH}} &= 0. \end{aligned} \quad [\text{Momentum basis}] \quad (1.10)$$

We now have enough information to make two very important insights about neutrinos in the SM.

The first important insight is that the chirality and helicity of the neutrino are the same for $m \rightarrow 0$. A particle's helicity is the projection of the spin vector on its momentum vector given as

$$\mathcal{H} = \frac{\boldsymbol{\sigma} \cdot \mathbf{P}}{|\mathbf{P}|} \quad (1.11)$$

where $\boldsymbol{\sigma}$ is the spin vector and \mathbf{P} is the 3-momentum of the particle. Since (1.10) commutes ($[\hat{A}, \hat{B}] = \hat{A}\hat{B} - \hat{B}\hat{A}$) with \mathcal{H} , $\psi_{\text{LH,RH}}$ are eigenstates of the helicity operator with eigenvalues ± 1 .

The second important fact is that a weakly interacting neutrino has positive energy $E = |\mathbf{P}|c$ and is always LH as shown in (1.6). The antineutrino is RH and has negative

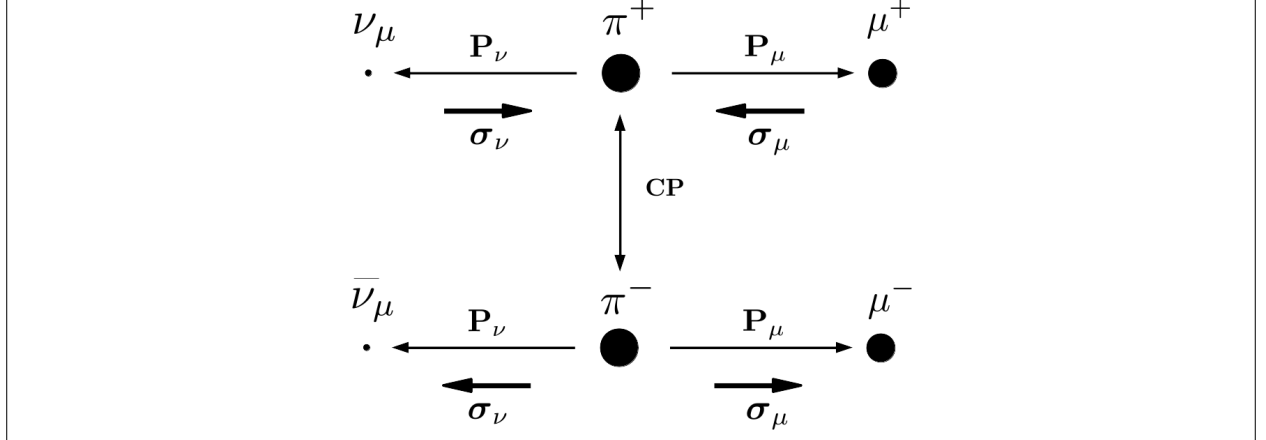


Figure 1.3: Decay of a charged pi meson into a muon and neutrino show the direction of the momentum \mathbf{P} and spin $\boldsymbol{\sigma}$ of the outgoing particles. Since a pion at rest has zero (0) angular momentum, the system of daughter particles must have net zero angular momentum as well. A neutrino (antineutrino) is a right- (left-) handed helicity particle since its spin is (anti-)parallel to its momentum. Application of charge and parity (CP) converts all the particles into their respective antiparticles.

energy ($-E = |\mathbf{P}|c$) which is interpreted to mean it travels backwards in time. Since neutrinos are nearly massless, there are no mechanisms for RH neutrinos and LH antineutrinos. The helicity of the neutrino is visualized in Figure 1.3 on page 8 which shows the decay of a pion at rest into a muon and neutrino. Since a pion has net zero (0) spin, the spin vectors of the daughters must also sum to zero. The neutrino's helicity (-1) and hence LH chirality is inferred by the positively charged muon of which has +1 helicity. To confirm the antineutrino's RH chirality (+1) requires both a charge (C) conjugation and parity (P) transformation. A C conjugation transforms all particles into their corresponding antiparticles while P transformation inverts all spatial coordinates.

The observation of only LH neutrinos and RH antineutrinos are an important feature in the SM. The weak force allows for P and CP violation due to its vector minus axial-vector (V-A) construction which is how a LH neutrino is described in (1.6). Further observation of CP violation is being explored with neutrinos through a process called neutrino oscillations. This will be explained in the next subsection.

1.1.2 Neutrino Oscillations

Neutrino oscillations are the observation of a neutrino produced of definite flavor and later observed as a different flavor. A deficit of neutrinos were observed for a number of atmospheric and solar neutrino experiments and the effect became more pronounced as the distance from the source increased. Oscillations established that one or more neutrinos have non-zero mass.

The first indication of neutrino oscillations was from the Ray Davis Homestake Mine experiment which began in the 1960s. Ray Davis was an expert Chemist and designed a radiochemical experiment to measure the flux of neutrinos from Sun. The purpose of this experiment was to test John Bahcall's prediction of the fusion rate in and neutrino flux from the Sun. Measurements continued into the 1980s and showed that the flux of neutrinos as measured at Homestake was about 1/3 the expected rate and became known as the "Solar Neutrino Problem." The primary solutions were either the neutrino capture cross section is lacking or the solar model was incorrect. The Sudbury Neutrino Observatory (SNO) was able to resolve this by making a model-independent measurement of the solar neutrino flux. The SNO ν_e CC/NC ratio is given by 0.301 ± 0.033 , which confirmed that only 30% of neutrinos arrive as ν_e on Earth, firmly established that the majority of neutrinos arrive as the wrong flavor [21].

Another outstanding problem emerged with measurements of atmospheric neutrinos, in particular muon and electron types. Atmospheric neutrinos are produced when high energy cosmic rays strike atmospheric particles. These cosmic ray collisions generate mostly pions and kaons that decay into neutrinos. When trying to measure the ν_μ/ν_e ratio and comparing that with expected ratio, there was a significant deficit. This was particularly a problem as a function of the zenith angle for the Super-Kamiokande experiment. It was the first experiment to perform a neutrino oscillation analysis that successfully explained the deficit.

While the phenomenon of neutrino oscillations has been understood for decades, it is not incorporated formally into the SM since oscillations require the neutrino has mass. The reasons why neutrino oscillations require massive neutrinos is explained in the next subsection.

1.1.2.1 Two Flavor Derivation

The phenomenon of neutrino oscillations can be described with elementary Quantum Mechanics. Beginning with the Schrödinger Equation in (1.12)

$$-\frac{\hbar}{i} \frac{\partial}{\partial t} |\nu(\mathbf{r}, t)\rangle = \hat{H} |\nu(\mathbf{r}, t)\rangle \quad (1.12)$$

where \hat{H} is the Hamiltonian for the physical system. If we consider a massive neutrino of mass m_j in its rest frame (free particle), the Hamiltonian becomes diagonal which acting on $|\nu_j\rangle$ results in the eigenvalue equation

$$\hat{H} |\nu_j(\mathbf{r}, t)\rangle = E_j |\nu_j(\mathbf{r}, t)\rangle \quad (1.13)$$

where E_j is the energy of the neutrino $|\nu_j\rangle$. If we substitute (1.13) into (1.12) and solve for $|\nu(\mathbf{r}, t)\rangle$, we obtain the following

$$|\nu_j(\mathbf{r}, t)\rangle = e^{-iE_j t/\hbar} |\nu_j(\mathbf{r}, t=0)\rangle \quad (1.14)$$

where $|\nu_j(\mathbf{r}, t=0)\rangle$ is created with momentum \mathbf{p} at the origin $\mathbf{r} = 0$. The time-independent solution to (1.12) is a plane-wave given by

$$|\nu_j(\mathbf{r}, t=0)\rangle = e^{i\mathbf{p} \cdot \mathbf{r}/\hbar} |\nu_j\rangle. \quad (1.15)$$

Before being able to describe neutrino oscillations, we must define our basis states. For this example, consider that there are only two eigenstates, labeled ν_1 and ν_2 , in the “mass” basis with definite mass m_1 and m_2 , respectively. However, experiments can produce neutrinos, as

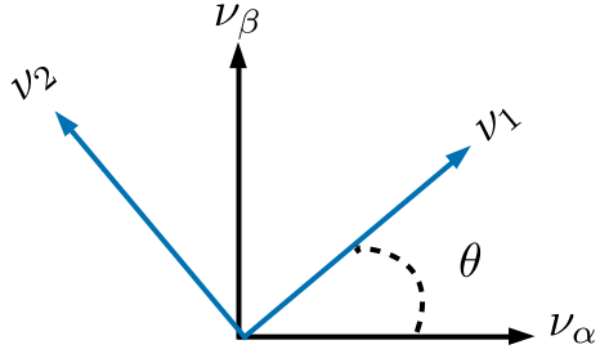


Figure 1.4: The depiction of two neutrino flavor change of basis using a rotation matrix. Compare this with (1.17).

well as probe them, only of definite “flavor”, denoted by a Greek letter subscript λ . Let the generated neutrino, which is a linear superposition of mass states 1 and 2, have momentum \mathbf{p} and flavor α . Since both mass eigenstates share the same momentum \mathbf{p} (but not energy!), the exponential term in (1.15) is an overall phase that will cancel out later. We can postulate a linear transformation, U , between the basis states given by (1.16).

$$\begin{bmatrix} \nu_\alpha \\ \nu_\beta \end{bmatrix} = \begin{bmatrix} U_{11} & U_{12} \\ U_{21} & U_{22} \end{bmatrix} \begin{bmatrix} \nu_1 \\ \nu_2 \end{bmatrix} \quad (1.16)$$

This linear transformation must be a unitary matrix ($U^{-1} = U^\dagger$, \dagger = transpose conjugate) since the states $\nu_{1,2}$ constitute a complete orthonormal set in the mass basis. With this unitary property, we can imagine U as a rotation matrix

$$\begin{bmatrix} \nu_\alpha \\ \nu_\beta \end{bmatrix} = \begin{bmatrix} \cos(\theta) & \sin(\theta) \\ -\sin(\theta) & \cos(\theta) \end{bmatrix} \begin{bmatrix} \nu_1 \\ \nu_2 \end{bmatrix}, \quad (1.17)$$

where θ is the angle between the two bases. We can imagine this transformation between bases as shown in Figure 1.4 on page 11 . If we create a neutrino of flavor α and observe it after a time $t = T > 0$, then the probability of observing it as flavor $\beta \neq \alpha$ is given by

$$\begin{aligned}
\mathcal{P}(\nu_\alpha \rightarrow \nu_\beta) &= \left| \langle \nu_\alpha(t=0) | \nu_\beta(t=T) \rangle \right|^2 \\
&= |(\cos(\theta) \langle \nu_1(t=0) | + \sin(\theta) \langle \nu_2(t=0) |) \\
&\quad \times (-\sin(\theta) | \nu_1(t=T) \rangle + \cos(\theta) | \nu_2(t=T) \rangle)|^2 \\
&= |\langle \nu_1(0) | \nu_1(T) \rangle (-cs) + \langle \nu_1(0) | \nu_2(T) \rangle (cc) \\
&\quad + \langle \nu_2(0) | \nu_1(T) \rangle (-ss) + \langle \nu_2(0) | \nu_2(T) \rangle (sc)|^2
\end{aligned} \tag{1.18}$$

where for simplicity $c = \cos(\theta)$ and $s = \sin(\theta)$. Evaluating all inner products and simplifying terms in (1.18) results in (1.19) below.

$$\mathcal{P}(\nu_\alpha \rightarrow \nu_\beta) = \sin^2(2\theta) \sin^2\left(\frac{E_1 - E_2}{2\hbar} T\right) \tag{1.19}$$

The terminology of “neutrino oscillations” should be more apparent now since (1.19) demonstrates that the probability changes sinusoidally. This equation is not, however, terribly useful in the laboratory frame since it is hard to make an experiment where the travel time an individual neutrino is well known. Instead, we can make useful approximations that are accessible in the laboratory frame. Since neutrinos are nearly massless, they travel very close to the speed of light. Therefore we can replace time T with L/c where L is the distance between the neutrino origin and detection and c is now the speed of light in vacuum. We can also approximate the energy of the mass eigenstate as

$$\begin{aligned}
E_j &= \left(m_j^2 c^4 + p_j^2 c^2\right)^{\frac{1}{2}} = p_j c \left(1 + \frac{m_j^2 c^2}{p_j^2}\right)^{\frac{1}{2}} \\
&\approx p_j c \left(1 + \frac{m_j^2 c^2}{2p_j^2} + \mathcal{O}\left(\frac{m_j c}{p_j}\right)^4\right) \\
&\approx E_\nu + \frac{m_j^2 c^4}{2E_\nu},
\end{aligned} \tag{1.20}$$

where we have used the fact that $p_j \gg m_j c$ and $p_j c \approx E_\nu$ where E_ν is the neutrino energy as measured in the laboratory. Substituting all of our assumptions in (1.19), we get (1.21)

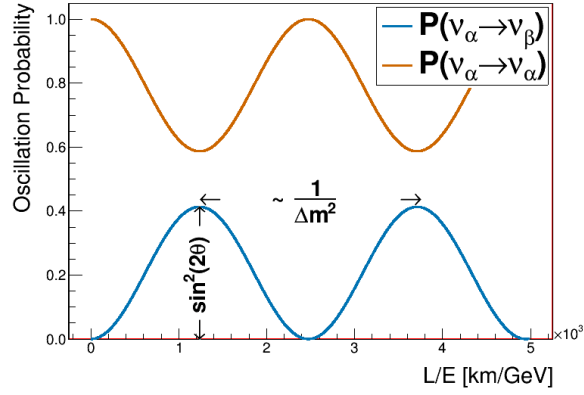


Figure 1.5: Two flavor oscillation probability as a function L/E is shown using $\theta = 20^\circ$ and $\Delta m^2 = [10^{-3}]eV^2$. The spacing between adjacent peaks/troughs is proportional to the inverse of Δm^2 . Note that $\mathcal{P}(\nu_\alpha \rightarrow \nu_\alpha) = 1 - \mathcal{P}(\nu_\alpha \rightarrow \nu_\beta)$ since the oscillation probability must always sum to 1.

$$\mathcal{P}(\nu_\alpha \rightarrow \nu_\beta) = \sin^2(2\theta) \sin^2\left(\frac{\Delta m^2 c^3}{4\hbar} \frac{L}{E_\nu}\right), \quad (1.21)$$

where $\Delta m^2 = m_2^2 - m_1^2$ is the mass-squared difference between the mass states. If we evaluate all the physical constants in natural units ($c = \hbar = 1$) and choose appropriate units for Δm^2 , L , and E_ν , we arrive at the following expression

$$\mathcal{P}(\nu_\alpha \rightarrow \nu_\beta) = \sin^2(2\theta) \sin^2\left(1.27 \frac{\Delta m^2}{[\text{eV}^2]} \frac{L/E_\nu}{[\text{km/GeV}]}\right) [\text{natural units}] \quad (1.22)$$

which more clearly demonstrates the Physics in oscillations. The oscillation probability has an amplitude of $\sin^2(2\theta)$ and varies with frequency inversely proportional to Δm^2 as illustrated in Figure 1.5 on page 13. Since L and E_ν are the only controllable parameters for an oscillation experiment, probing θ or Δm^2 can be difficult unless the experiment can probe a large range of L/E_ν as shown in Figure 1.6 on page 14.

1.1.2.2 Three Flavor Oscillations

In the general case of oscillations using a $n \times n$ mixing matrix, the unitary transformation can be written as a rotation matrix with $\frac{n}{2}(n-1)$ weak mixing angles with $\frac{1}{2}(n-2)(n-1)$

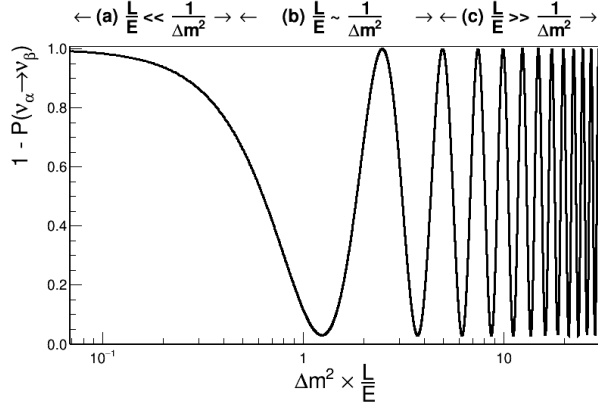


Figure 1.6: Logarithmic plot of the survival probability ($1 - \mathcal{P}(\nu_\alpha \rightarrow \nu_\beta) = \mathcal{P}(\nu_\alpha \rightarrow \nu_\alpha)$) over a wide range of L/E values for $\theta = 40^\circ$. The arrows above the plot roughly denote three possible cases: (a) no oscillations ($L/E \ll 1/\Delta m^2$); (b) sensitivity to oscillations ($L/E \sim 1/\Delta m^2$); (c) only average measurement ($L/E \gg 1/\Delta m^2$). Image originally inspired by [17].

Charge-Parity (CP) violating phases. In addition, oscillations are dictated by a total of $n - 1$ mass-squared splittings [21]. This all assumes that neutrinos obey the Dirac Equation, or that they are not their own antiparticles. The flavored mixing model is the 3×3 matrix since there are three known neutrino flavors, ν_e , ν_μ , and ν_τ , which means there are three (3) mixing angles, one (1) CP violating phase, and two (2) mass-squared splittings.

The most frequently used matrix parameterization is the MNSP (MNSP: Maki-Nakagawa-Sakata-Pontecorvo) matrix. Pontecorvo is accredited for first conceiving of neutrino oscillations, albeit between neutrino and anti-neutrinos [14]. It was Maki, Nakagawa, and Sakata who conceived of the parameterization based off the ideas of Pontecorvo [13]. The MNSP matrix is decomposed into separate rotation matrices as given by (1.23)

$$U_{\text{MNSP}} = \overbrace{\begin{bmatrix} 1 & 0 & 0 \\ 0 & c_{32} & s_{32} \\ 0 & -s_{32} & c_{32} \end{bmatrix}}^{U_{\text{atm}}} \times \overbrace{\begin{bmatrix} c_{31} & 0 & s_{31}e^{i\delta_{\text{CP}}} \\ 0 & 1 & 0 \\ -s_{31}e^{-i\delta_{\text{CP}}} & 0 & c_{31} \end{bmatrix}}^{U_{\text{rea}}} \times \overbrace{\begin{bmatrix} c_{21} & s_{21} & 0 \\ -s_{21} & c_{21} & 0 \\ 0 & 0 & 1 \end{bmatrix}}^{U_{\text{sol}}} \quad (1.23)$$

where

$$c_{ij} = \cos \theta_{ij}, s_{ij} = \sin \theta_{ij}, \quad (1.24)$$

Source	Species	Baseline [km]	Mean Energy [GeV]	$\min(\Delta m^2)$ [eV ²]
Reactor	$\bar{\nu}_e$	1	$\sim 10^{-3}$	$\sim 10^{-3}$
Reactor	$\bar{\nu}_e$	100	$\sim 10^{-3}$	$\sim 10^{-5}$
Accelerator	$\nu_\mu, \bar{\nu}_\mu$	1	~ 1	~ 1
Accelerator	$\nu_\mu, \bar{\nu}_\mu$	10^3	~ 1	$\sim 10^{-3}$
Atmospheric ν 's	$\nu_{e,\mu}, \bar{\nu}_{\mu,e}$	10^4	~ 1	$\sim 10^{-4}$
Sun	ν_e	1.5×10^8	$\sim 10^{-3}$	$\sim 10^{-11}$

Table 1.1: Sensitivity of different oscillation experiments originally published in [19].

and δ_{CP} represents the CP violating phase. Each rotation matrix represents the different sources for neutrino oscillations experiments with “atm”, “rea”, and “sol” representing atmospheric ν 's, nuclear reactor ν 's, and Solar ν 's, respectively. The sensitivity of neutrino oscillations for different sources is given in Table 1.1 on page 15.

If neutrinos are their own antiparticles, they do not follow the Dirac Equation but do follow the Majorana Equation. This adds two (in general $n - 1$) more CP violating phases to the MNSP matrix in (1.23)

$$U_{\text{MNSP}} \rightarrow U_{\text{MNSP}} \times \overbrace{\begin{bmatrix} 1 & 0 & 0 \\ 0 & e^{i\alpha} & 0 \\ 0 & 0 & e^{i\beta} \end{bmatrix}}^{U_{\text{Majorana}}} \quad (1.25)$$

Unfortunately, neutrino oscillations are not able to probe the Majorana phases since the Majorana matrix is diagonal. The question of if neutrinos are Majorana ($\nu = \bar{\nu}$) or Dirac ($\nu \neq \bar{\nu}$) particles is an open question and is being explored by non-oscillation experiments. The full three flavor oscillation probability is given by

$$\begin{aligned} \mathcal{P}(\nu_\alpha \rightarrow \nu_\beta) = & \delta_{\alpha\beta} - 4 \sum_{j=1}^3 \left[\sum_{i>j}^3 \text{Re}(K_{\alpha\beta,ij}) \sin^2(\phi_{ij}) \right] \\ & + 4 \sum_{j=1}^3 \left[\sum_{i>j}^3 \text{Im}(K_{\alpha\beta,ij}) \sin(\phi_{ij}) \cos(\phi_{ij}) \right] \end{aligned} \quad (1.26)$$

where

$$K_{\alpha\beta,ij} = U_{\alpha i} U_{\beta i}^* U_{\alpha j}^* U_{\beta j} \quad (1.27)$$

encapsulates the MNSP matrix elements and

$$\phi_{ij} = \frac{\Delta m_{ij}^2 c^3}{4\hbar} \frac{L}{E_\nu}. \quad (1.28)$$

Since CP violation means that $\mathcal{P}(\nu_\alpha \rightarrow \nu_{\beta \neq \alpha}) \neq \mathcal{P}(\bar{\nu}_\alpha \rightarrow \bar{\nu}_{\beta \neq \alpha})$, CP violating (conserving) terms must be an odd (even) function of δ_{CP} . Consider the following examples, muon neutrino disappearance and muon neutrino to electron neutrino appearance.

Muon Neutrino Disappearance The probability of a muon type neutrinos disappearing is given by

$$\begin{aligned} \mathcal{P}(\bar{\nu}_\mu \rightarrow \bar{\nu}_\mu) &= 1 - 4s_{23}^2 c_{13}^2 (V_{\cos \delta_{\text{CP}}}) \sin^2 \phi_{31} \\ &\quad - 4s_{23}^2 c_{13}^2 (Z_{\cos \delta_{\text{CP}}}) \sin^2 \phi_{32} \\ &\quad - 4(V_{\cos \delta_{\text{CP}}}) (Z_{\cos \delta_{\text{CP}}}) \sin^2 \phi_{21} \end{aligned} \quad (1.29)$$

where

$$V_{\cos \delta_{\text{CP}}} = s_{12}^2 c_{23}^2 + s_{13}^2 s_{23}^2 c_{12}^2 + 2s_{12}s_{13}s_{23}c_{12}c_{23} \cos \delta_{\text{CP}} \quad (1.30)$$

$$Z_{\cos \delta_{\text{CP}}} = c_{12}^2 c_{23}^2 + s_{13}^2 s_{23}^2 s_{12}^2 - 2s_{12}s_{13}s_{23}c_{12}c_{23} \cos \delta_{\text{CP}} \quad (1.31)$$

and $\bar{\nu}_\mu$ represents either ν_μ or $\bar{\nu}_\mu$. Since all CP violating terms in (1.29) are even functions of δ_{CP} , this channel does not offer insights into CP violation in a vacuum⁴.

Electron Neutrino Appearance While CP violation is not observable in muon neutrino disappearance, it is with electron neutrino appearance. The appearance probability of electron neutrinos types from muon types is given by

⁴When going to through matter however, the oscillation probability is affected. This is explained more in Section 1.1.2.3.

Parameter	Normal Hierarchy value	Inverted Hierarchy value	Units
$\Delta m_{32}^2 = \Delta m_{\text{atm}}^2$	2.51 ± 0.05	-2.56 ± 0.04	10^{-3} eV^2
$\Delta m_{21}^2 = \Delta m_{\text{sol}}^2$		7.53 ± 0.18	10^{-5} eV^2
$\sin^2(\theta_{21}) = \sin^2(\theta_{\text{sol}})$		$0.307^{+0.013}_{-0.012}$	1
$\sin^2(\theta_{32}) = \sin^2(\theta_{\text{atm}})$	O1: $0.417^{+0.025}_{-0.028}$	O1: $0.421^{+0.033}_{-0.025}$	1
	O2: $0.597^{+0.024}_{-0.030}$	O2: $0.592^{+0.023}_{-0.030}$	
$\sin^2(\theta_{31})$		2.12 ± 0.08	10^{-2}
δ_{CP}	217^{+40}_{-28}	280^{+25}_{-28}	degrees

Table 1.2: Table of best fit MNSP parameters split by normal and inverted hierarchy. O1 and O2 correspond to the first octant ($\theta \in (0, \pi/2)$) or second octant ($\theta \in (\pi/2, \pi/4)$). All values except for δ_{CP} are combined values from the Particle Data Group and δ_{CP} is from the 2018 NuFit analysis [8, 19].

$$\begin{aligned}
\mathcal{P}(\bar{\nu}_\mu \rightarrow \bar{\nu}_e) = & 4c_{13}^2 s_{13}^2 s_{23}^2 \sin^2 \phi_{31} \\
& + 8 \left(X_{\cos \delta_{\text{CP}}} \right) \cos \phi_{23} \sin \phi_{31} \sin \phi_{21} \\
& - \underbrace{8 \left(Y_{\sin \delta_{\text{CP}}} \right)}_{\text{CP violating}} \sin \phi_{32} \sin \phi_{31} \sin \phi_{21} \\
& + 4 \left(Z_{\cos \delta_{\text{CP}}} \right) s_{12}^2 c_{13}^2 \sin^2 \phi_{21}
\end{aligned} \tag{1.32}$$

where

$$X_{\cos \delta_{\text{CP}}} = c_{13}^2 s_{12} s_{13} s_{23} (c_{12} c_{23} \cos \delta_{\text{CP}} - s_{12} s_{13}) \tag{1.33}$$

$$Y_{\sin \delta_{\text{CP}}} = \frac{1}{8} \sin(2\theta_{12}) \sin(2\theta_{13}) \sin(2\theta_{23}) c_{13} \sin \delta_{\text{CP}} \tag{1.34}$$

and (+) represents the sign change from neutrinos to antineutrinos. The CP violating term (1.34) is also known as the Jarlskog Invariant and is a measure of CP violation independent of the mixing parameterization [12]. This oscillation channel are of primary importance in accelerator and atmospheric neutrino oscillation experiments.

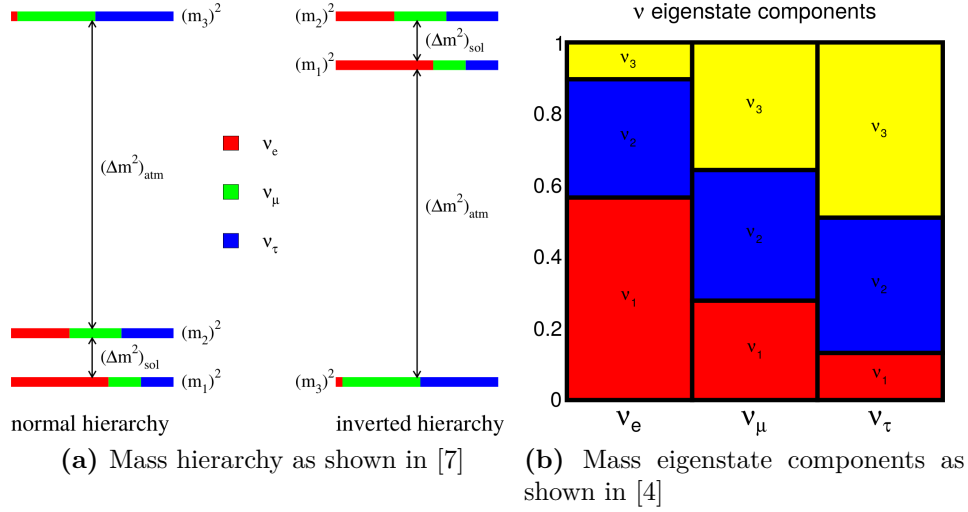


Figure 1.7: Left: the mass hierarchy problem is such that while the solar and atmospheric mixing mass-squared differences are clearly defined, the absolute mass scale is unknown. Since $m_2 > m_1$ by definition, it is currently unknown if m_3 is more or less massive than m_2 , or even massless! Notice the colored bars for each mass eigenstate which corresponded to the approximate flavor content of the neutrino. For example, state “2” has about equal three portions of all three flavors. Right: the mass eigenstate components of each flavor eigenstate. This is a complementary demonstration of the MNSP matrix.

Current and next generation experiments aim to improve knowledge of the mixing parameters. There are a couple of degeneracies to unravel as well as precise measurement of δ_{CP} . While the two defined mass-squared splittings $\Delta m_{21}^2 = \Delta m_{\text{sol}}^2$ and $\Delta m_{32}^2 = \Delta m_{\text{atm}}^2$ are known, it is unknown which eigenstates are more massive. This problem is known as the mass hierarchy problem and is illustrated in Figure 1.7a on page 18. Normal hierarchy refers to the case where $m_3 > m_2 > m_1$ whereas the inverted hierarchy has $m_2 > m_1 > m_3$. Also knowledge if θ_{23} is in the first octant $\theta \in (0, \pi/2)$ or second octant $\theta \in (\pi/2, \pi/4)$ requires large statistics. Finally the value of δ_{CP} is quite uncertain with values in the 3rd and 4th quadrants. Best fit measurements of the oscillations parameters is given in Table 1.2 on page 17.

1.1.2.3 Matter Effects

Traveling through matter also increases the sensitivity of oscillation measurements. Known as the Mikheyev-Smirnov-Wolfenstein (MSW) effect, all oscillations are affected by coher-

ent forward scattering of neutrinos with electrons in the media. Taking the example of $\langle \bar{\nu}_\mu \rangle \rightarrow \langle \bar{\nu}_e \rangle$ from (1.29), the MSW effect to first order is

$$\begin{aligned} \mathcal{P} \left(\langle \bar{\nu}_\mu \rangle \rightarrow \langle \bar{\nu}_e \rangle \right) \rightarrow & \mathcal{P} \left(\langle \bar{\nu}_\mu \rangle \rightarrow \langle \bar{\nu}_e \rangle \right) + \frac{8\alpha}{\Delta m_{31}^2} \left(c_{13}^2 s_{13}^2 s_{23}^2 \right) \left(1 - 2s_{13}^2 \right) \\ & \times \left(\sin^2 \phi_{31} - \underbrace{\left(\frac{\Delta m_{31}^2 c^3}{4\hbar} \frac{L}{E_\nu} \right)}_{\phi_{31}} \cos \phi_{32} \sin \phi_{31} \right) \end{aligned} \quad (1.35)$$

where

$$\alpha = 2\sqrt{2}G_F n_e E_\nu \quad (1.36)$$

and G_F is the Fermi constant and n_e is the average electron density of the Earth which the neutrinos travel [5]. Carefully studying 1.35 reveals that the MSW effect alters the oscillation probability as a function of the electron density and increases in magnitude with baseline.

1.1.3 CP Violation: Origins of Matter

To conclude the introduction on neutrinos, let's briefly examine the implications of CP violation. The observation of CP violation in the lepton sector might provide critical insight into the origins of the matter. CP violation dictates that certain interactions behave differently between matter or antimatter like $\mathcal{P} \left(\nu_\mu \rightarrow \nu_e \right) \neq \mathcal{P} \left(\bar{\nu}_\mu \rightarrow \bar{\nu}_e \right)$. The Big Bang Theory suggests that in the first fractions of a second of the Universe, equal amounts of matter and antimatter were created. However, observational evidence shows the Universe consists of baryonic matter (i.e. protons and neutrons). This is known as the Baryon Asymmetry of the Universe (BAU).

The process of Baryogenesis⁵ is a favored model to explain the BAU and lacks a necessary precursor mechanism. One of the necessary conditions for Baryogenesis [16] is C symmetry violation and CP violation. Evidence of CP violation has been experimentally confirmed in

⁵Baryogenesis is the mechanism by which matter and antimatter baryons are created in the early Universe.

the quarks, but not to the level which resolves the BAU. Baryogenesis can be achieved by having Leptogenesis⁶ occur first through the decay of very heavy, right handed Majorana neutrino ($\nu = \bar{\nu}$) through the *see-saw* mechanism. Detailed discussions on Leptogenesis and the *see-saw* mechanism can found in [4].

1.2 Tokai-to-Kamioka Experiment

The Tokai-to-Kamioka (T2K) experiment is a long baseline, neutrino oscillation experiment hosted in Japan [1] as shown in Figure 1.8 on page 21. It is the successor experiment to the KEK-to-Kamioka neutrino oscillation experiment also hosted in Japan. T2K produces its high intensity, muon neutrino pure beam at the Japan Proton Accelerator Complex (J-PARC), a world class particle accelerator facility. The beam is directed at the Super-Kamiokande (SK) [10] detector which is 295 km away from the source. Along the beamline at 280m from the beam source are a series of near detectors called ND280 [9] to observe and characterize the unoscillated beam. The beam is designed to maximize the $\nu_\mu \rightarrow \nu_e$ probability at the 295km baseline using a neutrino energy spectrum sharply peaked at 0.6GeV. This spectrum is achieved by directing the center of the beam 2.5 degrees from SK.

T2K was primarily designed to measure the last unknown MNSP mixing angle θ_{13} , which was thought to be nearly zero. In addition it set out to measure to high precision the atmospheric mixing parameters, θ_{23} and Δm_{23}^2 . One of its early successes was a landmark 7.3σ measurement of a non-zero θ_{13} using the electron-neutrino appearance measurement [2]. It continues to be a world leader in oscillation physics and as of 2018 rejects CP conserving values ($\delta_{\text{CP}} = 0, \pi$) at the 2σ level [3].

The following topics will be discussed in the following order. First a look how neutrinos are produced at J-PARC. Next a detailed look at the T2K near detectors which are used in

⁶Leptogenesis is the mechanism by which leptons and anti-leptons are created in the early Universe.

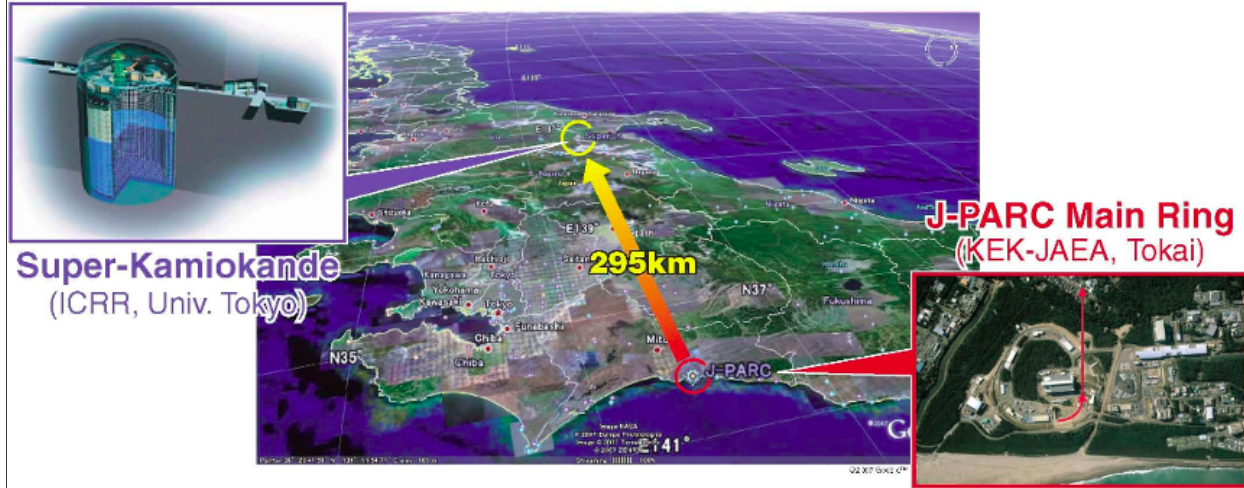


Figure 1.8: Birds eye view of the T2K experiment on the Japanese archipelago. An intense beam of neutrinos are produced at the J-PARC site (bottom right red box) using high energy protons. The beam is directed towards the Super-Kamiokande detector (top left blue box) at a distance of 295 km away from J-PARC.

this thesis. This is followed by a discussion on Super-Kamiokande, the T2K far detector. The final topic is the basics of an oscillation analysis using a near and far detector.

1.2.1 Neutrino Production at J-PARC

To facilitate the high intensity neutrino beam requirements for T2K, the J-PARC site generates a high intensity proton beam through a series of particle accelerators. A bird's eye view of J-PARC can be seen in Figure 1.9 on page 22 which highlights its different accelerators and facilities. For this section, note that all beam energies are kinetic energies.

Protons for the T2K beamline are first accelerated in the J-PARC linear accelerator⁷ (linac) and rapid cycle synchrotron⁸ (RCS). Protons are initially extracted from a hydrogen ion ($^1\text{H}^+$) source. Those protons are feed through a radio frequency (RF) quadrupole magnet and a series of linac elements as shown in 1.10a. Each linac element accelerates the protons

⁷A linear accelerator accelerates particles using time varying electric fields along a one direction, terminal beamline. Not only used in particle physics, they are also used in the medical field to generate X-rays.

⁸A synchrotron is cyclic particle accelerator that relies on time varying magnetic fields to accelerate particles. Since they require many magnets and large spaces to operate, they are usually operated at national laboratories for others uses as well like material and life sciences.

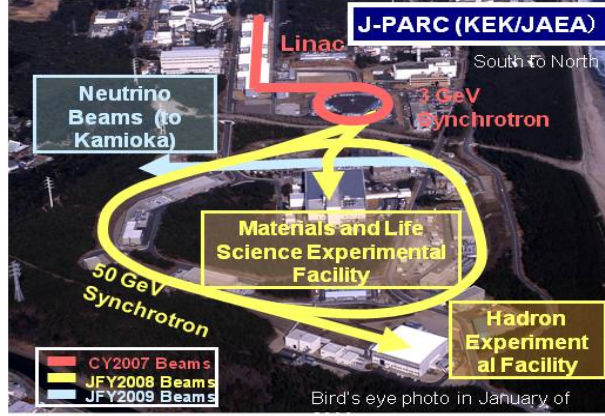


Figure 1.9: Bird’s eye view of the J-PARC center showing the primary components of its accelerator programs. To generate the high intensity neutrino beam, first the linear accelerator (Linac, red) accelerates hydrogen ions (protons) into the 3 GeV Synchrotron (also red) called the rapid-cycle synchrotron (RCS). The RCS then injects some of its protons into the 50 GeV Synchrotron (yellow) called the main ring (MR) which currently runs at 30 GeV. Finally the MR protons are directed into a target material along the neutrino beamline (teal) [6].

using carefully coordinated oscillating electric fields generated by RF pulses. After travelling 240m along the linac, the protons are boosted to 400 MeV and transported into the RCS. The 348m circumference RCS then further boosts the protons to 3 GeV at an operating frequency of 25 Hz. While being accelerated, protons are aggregated into two bunches and focused using particle collimators as shown in Figure 1.10b on page 23.

The next stage for the protons intended for the neutrino beamline is the much larger main ring (MR) synchrotron as shown in Figure 1.10c on page 23 which has a circumference of 1567m. While nominally designed to boost protons to 50 GeV, it currently operates at 30 GeV. Protons are injected into the MR to form eight proton bunches (spill), initially six when T2K first ran, before entering the neutrino beamline. The total temporal width of the spill is approximately $0.5\mu s$. [1]. At a spill cycle frequency of 0.5Hz, the bunches are extracted from the MR into the neutrino beamline.

The neutrino beamline is designed to direct the protons toward SK and generate neutrinos by impinging them on a cylindrical target. Figure 1.11a on page 24 shows the process of proton extraction from the MR for both primary and secondary neutrino beamlines. In the primary beamline, a series of normal and superconducting magnets steer the proton beam

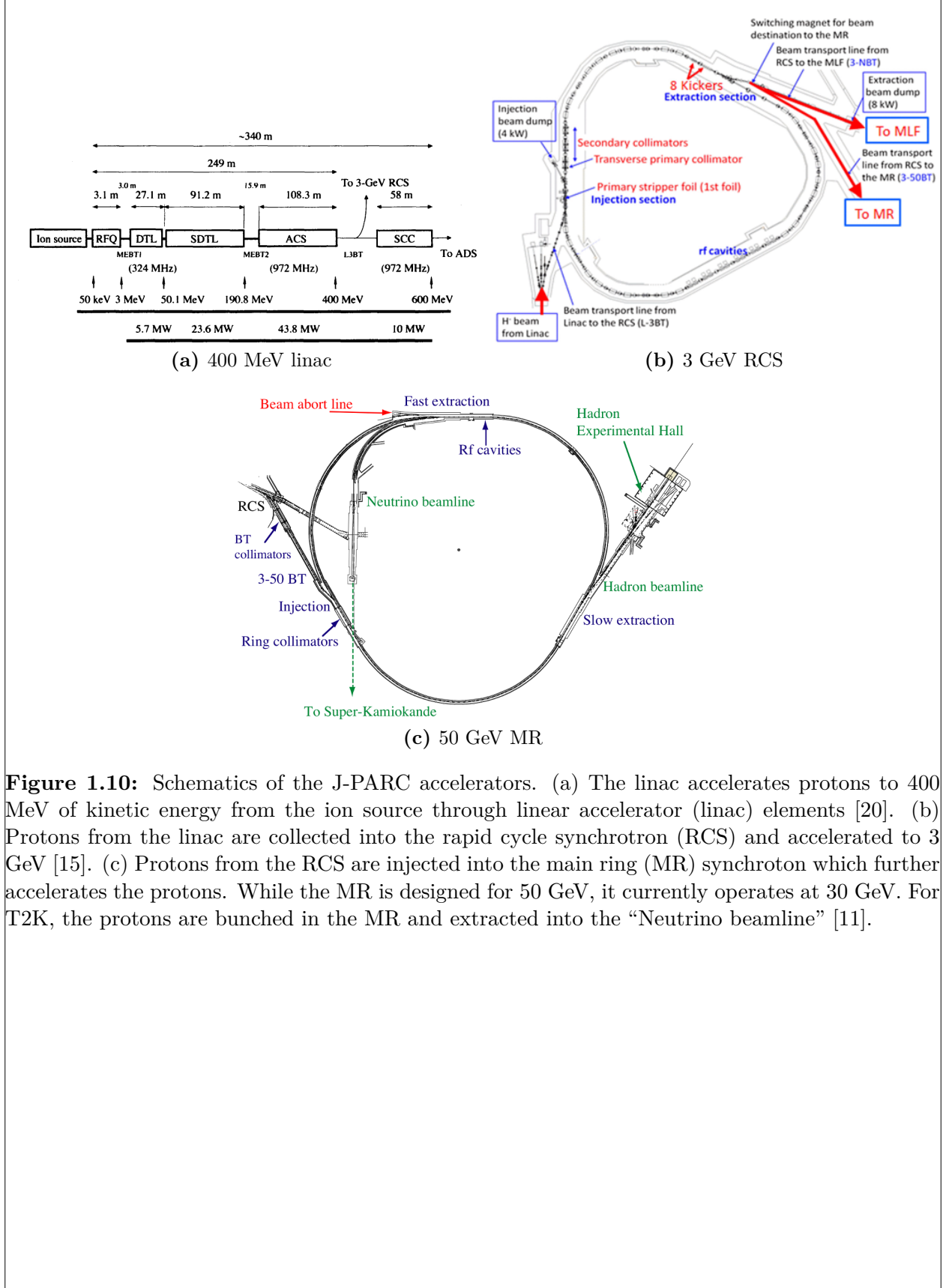


Figure 1.10: Schematics of the J-PARC accelerators. (a) The linac accelerates protons to 400 MeV of kinetic energy from the ion source through linear accelerator (linac) elements [20]. (b) Protons from the linac are collected into the rapid cycle synchrotron (RCS) and accelerated to 3 GeV [15]. (c) Protons from the RCS are injected into the main ring (MR) synchrotron which further accelerates the protons. While the MR is designed for 50 GeV, it currently operates at 30 GeV. For T2K, the protons are bunched in the MR and extracted into the “Neutrino beamline” [11].

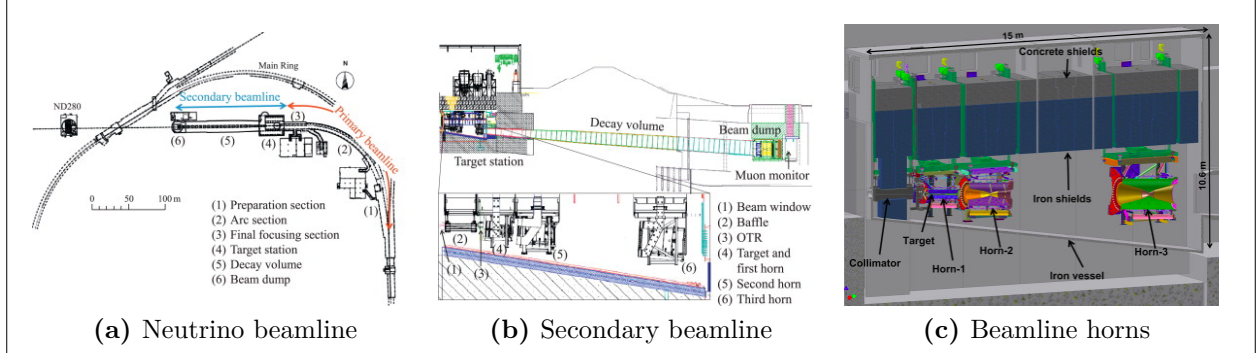


Figure 1.11: The neutrino beamline at J-PARC consists of a primary and secondary beamline. (a) The primary beamline redirects the protons towards the secondary beamline [1]. (b) In the secondary beamline, the protons are impinged on a cylindrical target producing mostly pions. The pions are focused using in sequence horns and decay in a long decay volume. Any non-decayed particles are stopped at the beam dump. (c) A further zoomed in cross section of the target station showing the target and focusing horns [18].

80.7° along a 104m radius of curvature. The secondary beamline, better shown in Figure 1.11b on page 24, illustrates the production of neutrinos. The beam spill impinges on a graphite target at the target station, which produces high energy pions like those produced from cosmic ray collisions in the upper atmosphere. To enhance the flux of neutrinos, a series of current pulsed, focusing magnets called horns⁹ as shown in Figure 1.11c on page 24 are used to focus pions of the correct charge towards SK. The horns are pulsed at +250kA (-250kA) to select positively (negatively) charged pions. The focused pions are allowed to decay along a 96m long decay volume to boost the daughter neutrinos along the beamline direction. The decay volume needs to be as close to vacuum as possible to reduce pion absorption and among other reasons, and thus it is filled with gaseous helium at 1 atm for safety reasons. Daughter muons of sufficient momentum (> 5 GeV) are further used to characterize the neutrino flux .

J-PARC continues to improve the MR proton delivery since T2K begin in 2010. T2K has run with both +250kA and -250kA horn currents with increasing beam power over time. Focusing positively charged pions with +250kA horn current is called forward horn current

⁹The name horn derives from the fact that the focusing magnets are shaped like brass horns in a music ensemble or marching band. One can think of these horns like a focusing lens for charged particles.

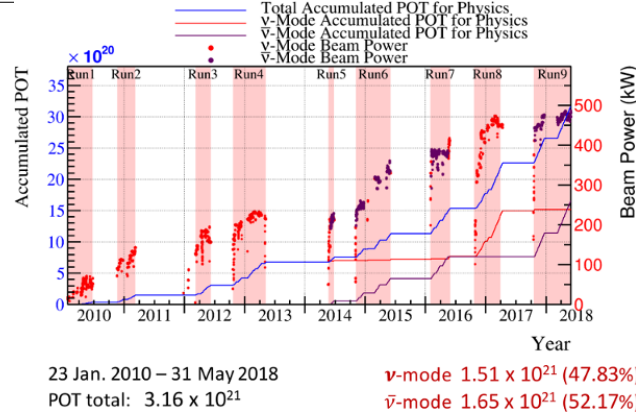


Figure 1.12: T2K accumulated protons on target since 2010 shows a steady increase in beam power over time. The gap between Run2 and Run3 is due to the damage suffered at J-PARC after the 2011 Tōhoku earthquake.

(FHC) mode or ν -mode. Similarly, using -250kA horn current is called reverse horn current (RHC) or $\bar{\nu}$ -mode. The aggregate running periods for T2K for both FHC and RHC are shown in Figure 1.12 on page 25 in units of protons on target (POT or PoT).

1.2.2 T2K Near Detectors

1.2.3 Far Detector: Super-Kamiokande

1.2.4 Oscillation Analysis

The number of reconstructed neutrino events of flavor α observed at the far detector (FD) is sum of all true charged current (CC) events $S_{\nu_\alpha}^{\text{FD}}$ and backgrounds B

$$N_{\nu_\alpha}^{\text{FD}} = S_{\nu_\alpha}^{\text{FD}} + B$$

where

$$\begin{aligned} S_{\nu_\alpha}^{\text{FD}} \rightarrow S_{\nu_\alpha}^{\text{FD}}(p_\alpha, \theta_\alpha; \vec{o}) &= \sum_i \sum_\beta \mathcal{P}_{\nu_\beta \rightarrow \nu_\alpha}(E_{\nu,i}; \vec{o}) \times \sigma_{\nu_\alpha}^{\text{CC}}(E_{\nu,i}) \\ &\times \Phi_{\nu_\alpha}^{\text{FD}}(E_{\nu,i}) \times T^{\text{FD}} \times \epsilon^{\text{FD}}(p_\alpha, \theta_\alpha) \end{aligned}$$

where

$$\sigma_{\nu_\alpha}^{\text{CC}}(E_\nu) = \sum_{\text{mode}} [\sigma(E_\nu)]_{\nu_\alpha \text{ CC mode}}$$

Bibliography

- [1] K. Abe et al. The T2K Experiment. *Nucl. Instrum. Meth.*, A659:106–135, 2011. 20, 22, 24
- [2] K. Abe et al. Observation of Electron Neutrino Appearance in a Muon Neutrino Beam. *Phys. Rev. Lett.*, 112:061802, 2014. 20
- [3] K. Abe et al. Search for CP Violation in Neutrino and Antineutrino Oscillations by the T2K Experiment with 2.2×10^{21} Protons on Target. *Phys. Rev. Lett.*, 121:171802, Oct 2018. 20
- [4] C. Adams et al. The Long-Baseline Neutrino Experiment: Exploring Fundamental Symmetries of the Universe. 2013. arXiv:1307.7335. 4, 18, 20
- [5] Jiro Arafune, Masafumi Koike, and Joe Sato. CP violation and matter effect in long baseline neutrino oscillation experiments. *Phys. Rev. D*, 56:3093–3099, Sep 1997. 19
- [6] J-PARC Center. What is J-PARC?, January 2019. <https://j-parc.jp/researcher/en/about/what/index.html>, Accessed on 26 January 2019. 22
- [7] A. de Gouvea et al. Working Group Report: Neutrinos. In *Proceedings, 2013 Community Summer Study on the Future of U.S. Particle Physics: Snowmass on the Mississippi*, 2013. arXiv:1310.4340. 18

-
-
- [8] I. Esteban et al. Global analysis of three-flavour neutrino oscillations: synergies and tensions in the determination of θ_{23} , δ_{CP} , and the mass ordering. 2018. arXiv:1811.05487. 17
- [9] A. Ferrero. The ND280 Near Detector of the T2K Experiment. *AIP Conference Proceedings*, 1189(1):77–82, 2009. 20
- [10] S. Fukuda et al. The Super-Kamiokande detector. *Nuclear Instruments and Methods in Physics Research Section A: Accelerators, Spectrometers, Detectors and Associated Equipment*, 501(2):418 – 462, 2003. 20
- [11] Susumu Igarashi. Recent Progress of J-PARC MR Beam Commissioning and Operation. In *Proceedings, 57th ICFA Advanced Beam Dynamics Workshop on High-Intensity and High-Brightness Hadron Beams (HB2016): Malmö, Sweden, July 3-8, 2016*, page MOAM6P60, 2016. 23
- [12] C. Jarlskog. A Basis Independent Formulation of the Connection Between Quark Mass Matrices, CP Violation and Experiment,. *Z. Phys.*, C29:491–497, 1985. 17
- [13] Z Maki, M. Nakagawa, and S. Sakata. Remarks on the Unified Model of Elementary Particles. *Progr. Theor. Exp. Phys.*, 28(5), 1962. 14
- [14] B. Pontecorvo. Inverse Beta Processes and Nonconservation of Lepton Charge. *J. Exp. Theor. Phys.*, 28(5), 1957. 14
- [15] P. K. Saha et al. Simulation, measurement, and mitigation of beam instability caused by the kicker impedance in the 3-GeV rapid cycling synchrotron at the Japan Proton Accelerator Research Complex. *Phys. Rev. Accel. Beams*, 21:024203, Feb 2018. 23
- [16] Andrei D Sakharov. Violation of CP invariance, C asymmetry, and baryon asymmetry of the universe. *Soviet Physics Uspekhi*, 34(5):392, 1991. 19
- [17] N. Schmitz. *Neutrinophysik*. Teubner, Stuttgart, 1997. 14

-
-
- [18] T. Sekiguchi et al. Development and operational experience of magnetic horn system for T2K experiment. *Nuclear Instruments and Methods in Physics Research Section A: Accelerators, Spectrometers, Detectors and Associated Equipment*, 789:57 – 80, 2015. 24
- [19] M. Tanabashi et al. The Review of Particle Physics. *Phys. Rev. D*, 98(030001), 2018. 15, 17
- [20] Y. Yamazaki, editor. *Accelerator technical design report for high-intensity proton accelerator facility project, J-PARC*. Number 2002-013. Japan Atomic Energy Research Institute, 2003. 23
- [21] Kai Zuber. *Neutrino Physics*. CRC Press, Boca Raton, FL., 2nd edition, 2012. 2, 9, 14